

Testing the effects from dark radiation

Yi Zhang ^{a,b,c1}, Yungui Gong ^{c,d2},

^a*College of Mathematics and Physics, Chongqing University of Posts and Telecommunications,
Chongqing 400065, China*

^b*High Energy Physics Division, Argonne National Laboratory,
Lemont, IL 60439, USA*

^c*Institute of Theoretical Physics, Chinese Academy of Science,
Beijing 100190, China*

^d*School of Physics, Huazhong University of Science and Technology,
Wuhan 430074, China*

Abstract

In this letter, the effects of dark radiation (DR) are tested. Theoretically, the phase-space analysis method is applied to check whether the model is consistent with the history of our universe which shows positive results. Observationally, by using the observational data (*SNLS* (SuperNovae Legacy Survey), *WMAP9* (Wilkinson Microwave Anisotropy Probe 9 Years Result), *PLANCK* (Planck First Data Release), *BAO* (Baryon Acoustic Oscillations), $H(z)$ (Hubble Parameter Data) and *BBN* (Big Bang Nucleosynthesis)), the dark radiation is found to have the effect of wiping out the tension between the *SNLS* data and the other data in flat Λ CDM model. The effects of dark radiation also make the best fit value of N_{eff} slightly larger than 3.04.

¹Email: zhangyia@cqupt.edu.cn

²Email: yggong@mail.hust.edu.cn

1 Introduction

The observations hint our universe is accelerating now (e.g. Refs. [1, 2, 3, 4, 5]). The observations also show a nearly flat universe with roughly 72% dark energy, 28% matter and 0.1% radiation (e.g. Refs.[6, 7, 8, 9, 10]). How to describe these observations by theories? The Λ CDM model is the simplest candidate. In Λ CDM model, the generation of neutrino is assumed as three. And, the number of the effective neutrino species is $N_{eff} = 3.04$ where the effects from the non-instantaneous neutrino decoupling from the primordial photon-baryon plasma are taken into account. However, many theoretical models indicate the existing of extra radiation, e.g. the FRW model in the Randall-Sundrum scenario [11, 12, 13, 14]; the Brans-Dicke theory [15, 16]; the Horava-Lifshitz theory [17, ?]; the decaying vacuum [19, 20, 21]; the negative Casimir effect [22].

Recently, the measurement of the temperature anisotropy of CMB (Cosmic Microwave Background) shows less power spectrum at small scale, suggesting that N_{eff} has a bigger value than the one predicted by the standard model of particle physics, so the existence of “dark radiation”. The results of *WMAP7* [10], *ACT* (the Atacama Cosmology Telescope [23, 24]) and *SPT* (South Pole Telescope [25]) give out the 1σ level of the effective neutrino number are $N_{eff} = 4.56 \pm 0.75$ (*WMAP7*), $N_{eff} = 2.78 \pm 0.55$ (*WMAP7*+*ACT*), 2.96 ± 0.44 (*WMAP7* + *ACT* + *SPT*); while the BBN data shows $N_{eff} = 3.24 \pm 0.6$ [26]. So many discussions on dark radiation have already appeared (e.g. Refs.[27, 28, 29, 30]).

In this letter, the Λ CDM model with dark radiation will be used to test the dark radiation effect which could be generated from a electroweak phase transition [31]. The letter is organized as follows. In Section 2, the model will be introduced. In Section 3, a phase-space analysis will be presented to get the evolution of our universe. Then in Section 4, we apply the observation data to test the model parameter space, including the *SNLS* complication of supernova Ia data [32, 33], the cosmic microwave background radiation data from *WMAP9* [34, 35] and *PLANCK* [36], the BAO distance measurements from the oscillations in the distribution of galaxies [37, 38, 39, 40], the Hubble parameter data [41, 42] and the BBN data [43, 44]. We will show the constraining results in Section 5. Finally, a short summary will be given out in Section 6.

2 The Model

Here, the geometry of space-time is assumed to be described by the FRW (Friedmann-Robertson-Walker) metric with a non-zero curvature,

$$ds^2 = -dt^2 + a^2(t) \left(\frac{dr^2}{1 - kr^2} + r^2(d\theta^2 + \sin^2 \theta d\varphi^2) \right), \quad (1)$$

where a is the scale factor, and k is the curvature parameter with the values of $0, \pm 1$ representing flat, closed and open spatial sector respectively.

The energy density components in our universe are represented by the pressureless matter part ρ_m , the dark energy part ρ_d , the ordinary radiation part ρ_r , the dark radiation part ρ_{dr} and the curvature part ρ_k . The Friedmann equation is

$$H^2 = \frac{1}{3m_{pl}^2} (\rho_m + \rho_d + \rho_r + \rho_{dr} + \rho_k), \quad (2)$$

where $\rho_k = -k/a^2$ and m_{pl} is the Planck mass. We call the Λ CDM model plus the dark radiation as the flat or curved dark radiation model. This kind of model could be derived from a quintessence scenario phenomenologically whose potential includes interactions of the field with virtual particles and the heat bath. As the potential is similar to the Higgs potential in the electroweak phase transition, a first-order phase transition at redshift $z \sim 3$ releases energy in relativistic model (dark radiation). After that, ρ_d becomes a constant; and the dark radiation appears [31].

After defining $\Omega_i = \rho_i/8\pi GH^2$, Ω_m , Ω_d , Ω_r , Ω_{dr} and Ω_k could represent the fractional energy densities for matter, dark energy, ordinary radiation, dark radiation and curvature respectively. The energy components are assumed to be conserved separately. Specially,

$$\Omega_r + \Omega_{dr} = \left[1 + \frac{7}{8} \left(\frac{4}{11} \right)^{\frac{4}{3}} N_{eff} \right] \Omega_\gamma, \quad (3)$$

where $h = H_0/100 \text{Mpc.km.s}^{-1}$, the index “0” denotes the present value of parameter and Ω_γ is the energy density of the CMB photons background at temperature $T_\gamma = 2.728K$. To represent the dark radiation, we use the symbols $f = \Omega_{dr0}/\Omega_{d0}$ which represents the ratio of today’s dark radiation and dark energy. Then, the Friedmann equation could be rewritten as below

$$H^2 = H_0^2 [\Omega_{d0} + \Omega_{k0} a^{-2} + \Omega_{m0} a^{-3} + \Omega_{r0} a^{-4} + f \Omega_{d0} a^{-4}]. \quad (4)$$

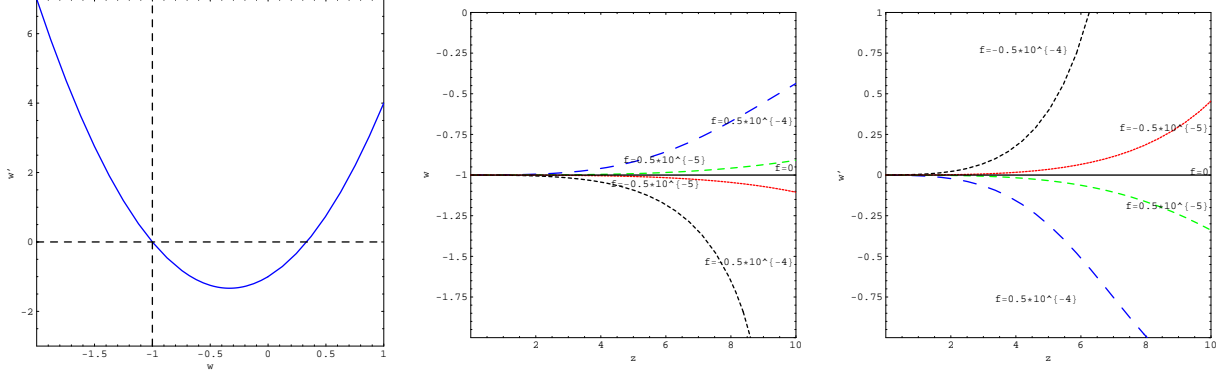


Figure 1: The left, middle and right panels are the relation of $\omega - \omega'$, $\omega - z$ and $\omega' - z$ separately.

If treating the dark radiation as a signal of dark energy, dark radiation leads to a characteristic time dependence in the effective EoS (equation of state) parameter of dark energy,

$$\omega(z) = \frac{p_d + p_{dr}}{\rho_d + \rho_{dr}} = \frac{f(1+z)^4/3 - 1}{f(1+z)^4 + 1}, \quad (5)$$

where z is the redshift with the definition $z = a^{-1} - 1$. And, the time derivative of the EoS parameter is

$$\omega' = -\frac{16}{3} \frac{f(1+z)^4}{[f(1+z)^4 + 1]^2}, \quad (6)$$

where a prime means the derivative with respect to $\ln a$. Based on Eqs.5 and 6, the relations of $\omega - \omega'$, $\omega - z$ and $\omega' - z$ are list in Figure 1. The curves show the deviations from the Λ CDM model are tiny with small f . Specifically, the knowledge of f is suffice to know the present value of EoS parameter where $1 + \omega_0 = +4f/3(1+f)$ and $\omega'_0 = -16f/3(1+f)^2$. If f is at the order of 10^{-5} , it is not surprising that the EoS parameter is very close to -1 and the derivative of the EoS parameter is tiny.

3 The Phase-Space Analysis

To do phase-space analysis in our model, three dimensionless parameters are defined firstly,

$$u = \sqrt{\frac{H_0^2 \Omega_{m0} a^{-3}}{H^2}}, \quad (7)$$

$$v = \sqrt{\frac{H_0^2 (\Omega_{r0} + \Omega_{dr0}) a^{-4}}{H^2}}, \quad (8)$$

$$w = \sqrt{\frac{H_0^2 \Omega_{k0} a^{-2}}{H^2}}. \quad (9)$$

Based the Friedmann equation and the conserved ones ³, the evolutions of u, v, w are

$$u' = u \left(-\frac{3}{2} + \frac{3}{2} u^2 + 2v^2 + w^2 \right), \quad (10)$$

$$v' = v \left(-2 + \frac{3}{2} u^2 + 2v^2 + w^2 \right), \quad (11)$$

$$w' = w \left(-1 + \frac{3}{2} u^2 + 2v^2 + w^2 \right). \quad (12)$$

When u', v' and w' are all equal to 0, the corresponding value of u, v, w gives a critical point. Four points are list in the Table 1. And, we could put a small perturbation near the critical points' neighbor. Then, the perturbation equations are gotten. If the real parts of the eigenvalues of the perturbation equations are all positive, the corresponding critical point is an unstable fixed point. In contrast, the negative real parts of the eigenvalues denotes a stable point. Specially if the real parts of the eigenvalues are mixed with the negative one and the positive one, the corresponding critical point is an unstable saddle point [46, 47, 48].

Generally speaking, the model with dark radiation could go through the unstable radiation dominated phase (R), the unstable matter dominated phase (M), the stable dark energy dominated phase (D) and the unstable curvature dominated phase (K) ⁴. The dark energy dominated phase is stable which means the universe will be dominated by the cosmological constant in the future. Before that, our universe is supposed to go through these unstable phases. This process is corresponding to the history of our universe: the radiation dominated phase at first, then matter dominated phase and finally the dark energy dominated phase.

³The conserved equation for each component is $\dot{\rho}_i + 3H\rho_i(1 + \omega_i) = 0$ where $\omega_r = 1/3$, $\omega_{dr} = 1/3$, $\omega_m = 0$ and $\omega_d = -1$.

⁴The unstable curvature dominated phase often represents some very early physics. Here, we ignore this phase on the discussions of the history of our universe.

Phase	Physical Meaning	(u, v, w)	Existing	$(\lambda_1, \lambda_2, \lambda_3)$	Stability
M	Matter Dominated	$(1, 0, 0)$	Always	$(3, -2, -1)$	Unstable
R	Radiation Dominated	$(0, \pm 1, 0)$	Always	$(\frac{3}{2}, 4, -1)$	Unstable
K	Curvature Dominated	$(0, \pm 1, 0)$	Always	$(-\frac{3}{2}, -2, 2)$	Unstable
D	Dark Energy Dominated	$(0, 0, 0)$	Always	$(-\frac{3}{2}, -2, -1)$	Stable

Table 1: We list the properties of the critical points: the physical meaning of the phases, the value of the phases, the existing condition, the eigenvalues of the points and the stability of the phases.

4 The Data and The Method Analysis

Once treating dark radiation as signal of dark energy, the observational testing method used in the dark energy model could be applied to test the dark radiation. In this section, the data and the analytical methods will be presented separately.

4.1 The Data Analysis

4.1.1 The *SNLS* data

SNe Ia (supernovae) is used in the standard distance method which measures the expansion of our universe. For the *SNLS* data, Ref. [32] gives the apparent B magnitude m_B , and the covariance matrix for $\Delta m \equiv m_B - m_{\text{mod}}$, with

$$m_{\text{mod}} = 5 \log_{10} D_L(z|\mathbf{s}) - \alpha(s - 1) + \beta \mathcal{C}_{SN} + \mathcal{M}, \quad (13)$$

where $D_L(z|\mathbf{s})$ is the luminosity distance multiplied by H_0 for a given set of cosmological parameters \mathbf{s} ⁵, \mathcal{C}_{SN} is the color measure for supernovae and \mathcal{M} is a nuisance parameter representing some combination of the absolute magnitude of a fiducial SNe Ia. The time dilation part of the observed luminosity distance depends on the total redshift z_{hel} [50]

$$D_L(z|\mathbf{s}) \equiv c^{-1} H_0 (1 + z_{\text{hel}}) r(z|\mathbf{s}), \quad (14)$$

where c is the color index, z and z_{hel} are the CMB rest frame and heliocentric redshifts of the supernovae. The correlated errors is

$$\chi_{SN}^2 = \Delta m^T \cdot \mathbf{C}_{SN}^{-1} \cdot \Delta m, \quad (15)$$

⁵ s is the stretch measure of the SNe Ia light curve shape.

where C_{SN} is the $N \times N$ covariance matrix of the SNe Ia where N is the number of the components. The nuisance parameter H_0 is marginalized over by evaluating χ_{SN}^2 .

4.1.2 The CMB Data

The CMB data is implemented to add distance measurements at higher redshift ($z > 10$). We use the derived quantities of the *WMAP9* and *PLANCK* measurements [60, 61]: the shift parameter $R(z^*)$, the acoustic scale $l_A(z^*)$ at the decoupling redshift and the base parameter ω_b whose definition is $\Omega_b h^2$ where Ω_b is the fractional energy densities for baryon. The χ^2 of CMB data is

$$\chi_{CMB}^2(\mathbf{p}, \Omega_b h^2, h) = \sum_{i,j=1}^3 \Delta x_i C_{CMB}^{-1}(x_i, x_j) \Delta x_j, \quad (16)$$

where the three parameters are $x_i = (R(z^*), l_A(z^*), \omega_b)$, $\Delta x_i = x_i - x_i^{obs}$ and $C_{CMB}(x_i, x_j)$ is the covariance matrix for the three parameters [10, 60, 61]. The shift parameter R is expressed as $R(z^*) = \left[\sqrt{\Omega_m} \text{sinn}(\sqrt{|\Omega_k|} \int_0^{z^*} dz/E(z)) \right] / \sqrt{|\Omega_k|} = 1.710 \pm 0.019$. The acoustic scale is $l_A(z^*) = \pi d_L(z^*) / (1 + z^*) r_s(z^*) = 302.1 \pm 0.86$. And the decoupling redshift z^* is fitted by Ref.[51] with $z^* = 1048[1 + 0.00124(\Omega_b h^2)^{-0.738}][1 + g_1(\Omega_m h^2)^{g_2}] = 1090.04 \pm 0.93$, where $g_1 = 0.0783(\Omega_b h^2)^{-0.238}[1 + 39.5(\Omega_b h^2)^{0.763}]$ and $g_2 = 0.560/[1 + 21.1(\Omega_b h^2)^{1.81}]$.

4.1.3 The BAO, $H(z)$ and BBN Data

To produce tightest cosmological constraint, we try to use other cosmological probes as well.

The *BAO* data are used as standard rule. Due to the sound waves in the plasma of the early universe, the wavelength of *BAO* is related to the co-moving sound horizon at the baryon drag epoch which is $d_z = r_s(z_d)/D_V(z)$, D_V is the effective distance with $D_V(z) = [z d_L^2(z)/H(z)(1+z)^2]^{1/3}$, z_d is the drag redshift defined in [49], and $r_s(z) = \int_z^\infty c_s(x) dx/E(x)$ is the co-moving sound horizon ⁶. For the BAO data, we use the measurements from the 6dFGS (hereafter Bao1) [40]), the distribution of galaxies (hereafter Bao2) [38] and the WiggleZ dark energy survey (hereafter Bao3) [39]. The 6dFGS (Bao6dF) gives

$$\chi_{Bao1}^2 = \frac{(d_{0.106} - 0.336)^2}{0.015^2}. \quad (17)$$

⁶ The sound speed is $c_s(z) = 1/\sqrt{3[1 + \bar{R}_b/(1+z)]}$ where $\bar{R}_b = 3\Omega_b h^2/(4 \times 2.469 \times 10^{-5})$.

And, the distribution of galaxies (Bao2) measured the distance ratio at two redshifts $z = 0.2$ and $z = 0.35$, whose χ^2 is

$$\chi_{Bao2}^2 = \sum_{i,j=1}^2 \Delta d_i C_{dz}^{-1}(d_i, d_j) \Delta d_j \quad (18)$$

where $d_i = (d_{z=0.2}, d_{z=0.35})$, $\Delta d_i = d_i - d_i^{obs}$ and the covariance matrix $C_{dz}(d_i, d_j)$ for d_z at $z = (0.2, 0.35)$ is taken from Eq. 5 in Ref.[38]. Furthermore, the WiggleZ dark energy survey measured the acoustic parameter $A(z) = D_V(z) \sqrt{\Omega_m H_0^2}/z$ at three redshifts $z = 0.44$, $z = 0.6$ and $z = 0.73$, and the results and their covariance matrix are listed in Table 2 and Table 3 of Ref.[39]. The χ^2 is

$$\chi_{Bao3}^2 = \sum_{i,j=1}^3 \Delta A_i C_A^{-1}(A_i, A_j) \Delta A_j, \quad (19)$$

where $A_i = [A(0.44), A(0.6), A(0.73)]$, $\Delta A_i = A(z_i) - A(z_i)^{obs}$. Then, the total χ^2 for *BAO* is

$$\chi_{Bao}^2(\mathbf{p}, \Omega_b h^2, h) = \chi_{Bao1}^2 + \chi_{Bao2}^2 + \chi_{Bao3}^2. \quad (20)$$

To alleviate the double integration of the EoS parameter $\omega(z)$, we also apply the measurements of the Hubble parameter $H(z)$ which could better constrain $w(z)$ at high redshift. We use the $H(z)$ data at 11 different redshifts obtained from the differential ages of red-envelope galaxies in Ref.[41], and three more Hubble parameter data $H(z = 0.24) = 76.69 \pm 2.32$, $H(z = 0.34) = 83.8 \pm 2.96$ and $H(z = 0.43) = 86.45 \pm 3.27$ determined by Ref.[42]. Then, the χ^2 of Hubble parameter data is

$$\chi_H^2(\mathbf{p}, h) = \sum_{i=1}^{14} \frac{[H(z_i) - H_{obs}(z_i)]^2}{\sigma_{hi}^2}, \quad (21)$$

where σ_{hi} is the 1σ uncertainty in the $H(z)$ data.

Furthermore, the constraint data from *BBN* is added for this dark radiation model. The χ^2 of the Big Bang Nucleosynthesis (*BBN*) data [43, 44, 45]) is

$$\chi_{bbn}^2 = \frac{(\Omega_{b0} h^2 - 0.022)^2}{0.002^2}, \quad (22)$$

where $\Omega_{b0} = 0.02253h^2$ is the present value of dimensionless energy density for baryon.

4.1.4 Data Discussion

To use the data properly, the *SNLS* data will be used individually at first and be denoted as “Data I”. To utilize the *WMAP9* and *PLANCK* data separately, we treat *WMAP9* + *BAO* + *H(z)* + *BBN* and *PLANCK* + *BAO* + *H(z)* + *BBN* as “Data II” and “Data III”. If all the three data are consistent, then we combine them as “Data IV: *SNLS* + *WMAP9* + *PLANCK* + *BAO* + *H(z)* + *BBN*”.

4.2 The Analysis Method

Monte Carlo Markov Chain (MCMC) method is used to compute the likelihood for the parameters in the model. By using the Metropolis-Hastings algorithm, the MCMC method randomly chooses values for the parameters, evaluates χ^2 and determines whether to accept or reject the set of parameters.

4.2.1 The AIC Principle

After combining different data, the total χ^2 could be gotten by adding all the observation’s χ^2 together. The model parameters are determined by minimizing χ^2 . To value the goodness of fitting, the *AIC* (Akaike Information Criterion) principle will be used which is very popular in Mathematics and Physics [62, 63],

$$AIC = \chi_{min}^2 + 2n, \tag{23}$$

where n is the number of parameters and χ_{min}^2 is the minimum value of χ^2 . The smaller the *AIC* value is, the better the constraint is. If the χ^2 difference between two models is in a range of $0 < \Delta(AIC) < 2$, the constraints of the two models are considered to be equivalent.

4.2.2 The Om Diagnostic

The Om diagnostic [52, 53] is proposed to distinguish dynamical dark energy from the cosmological constant both with and without the matter density. In another saying, it is on the basis of observations of the expansion history. The Om diagnostic could be

characterized by

$$Om(x) = \frac{H^2(x)/H_0^2 - 1}{x^3 - 1}, \quad x = 1 + z. \quad (24)$$

5 The Fitting Results

5.1 The Flat and Curved Λ CDM Model

To a certain model, different data may give out very different constraining results which is called tension. One reason of tension is the system error of different data. The other reason could be traced to the model which may not represent the true physics.

For flat Λ CDM model, Table 2 shows the 1σ upper bound of Ω_{m0} given by the SNLS data is 0.265 which is incompatible with the 1σ lower bound of Ω_{m0} given by Data III where $\Omega_{m0} = 0.270$. In another saying, the constraining parameter range from the two Data sets are not overlapped at 1σ level. For Data II, this situation are slightly better where the lower bound of Ω_{m0} is 0.252. Anyway, that is just slightly overlapped with the SNLS data. Tension exists between the *SNLS* data and the other data (including *WMAP9*, *PLANCK*, $H(z)$ and *BBN*). And, we could not combine all the data together for flat Λ CDM model.

Fortunately, after adding the curvature, Table 2 shows all the data are consistent. The 1σ range values of Ω_{m0} are overlapped and the tensions between the *SNLS* data and the other data are disappeared. Thus, it is reasonable to combine Data I, II and III to get tighter constraints for the curved Λ CDM model. Comparing the flat and curved Λ CDM model, $\Delta(AIC) = 1.67 < 2$; so the constants of the two models are considered to be equivalent. This tension resolution hints the system error of the data may not the reason. Refs.[58, 59] show that the assumption of a flat universe induces critically large errors in reconstructing the dark energy equation of state even if the true cosmic curvature is very small. As the dark radiation is also a small component, in the following, we will try to answer the question that whether the dark radiation part could alleviated the tension problem or not based on observations⁷.

⁷ The effect that extra radiation can smash off the data tension are reported for other observational data, e.g. [54, 55, 56, 57].

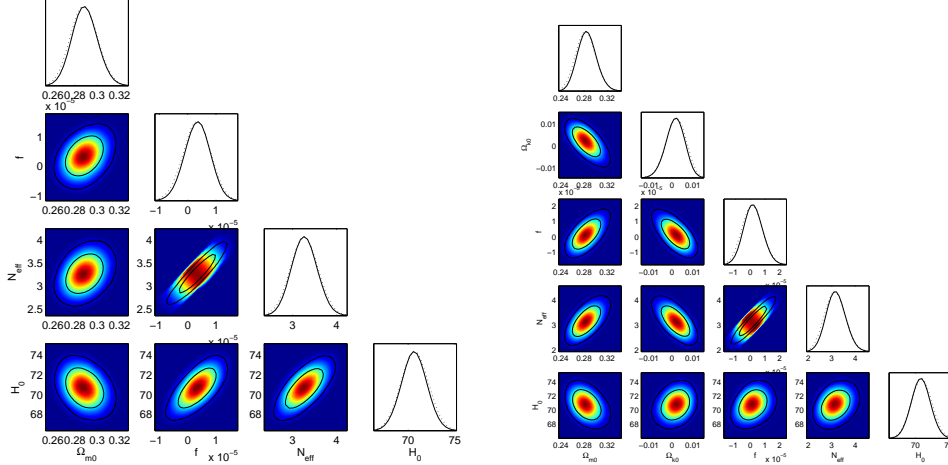


Figure 2: The constraining results of the flat and curved dark radiation models are presented in the left and right panels separately? The results are given by the $SNLS + WMAP9 + PLANCK + BAO + H(z) + BBN$ data (Data IV).

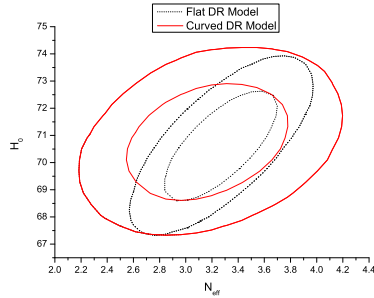


Figure 3: The contours for H_0 and N_{eff} are given out.

5.2 The Flat and Curved Λ CDM Model with Dark Radiation

After adding the dark radiation to the Λ CDM model, Table 2 shows $SNLS$ data gives a loose parameter range. As we expected, this tension problem is disappeared. Therefore, it is reasonable to use the combined $SNLS + WMAP9 + PLANCK + BAO + H(z) + BBN$ data. It gives out the tightest constraints. Then, what results could we get if we add both the curvature and the dark radiation to the Λ CDM model? As shown in Figure 2, the parameter ranges of the curved one are slightly enlarged compared to the flat one.

Generally speaking, the $SNLS$ data gives very poor constraints on the model parameter compared to other data. Data II, III and IV present $\Omega_{k0} \sim 10^{-2}$ and $f \sim 10^{-5}$ which denote the price we paid for the disappeared tension is reasonable. The AIC analysis also shows

the constraints on both the flat and curved ones are equal because the $\Delta(AIC)$ is less than 2. Anyway, the *PLANCK* + *BAO* + $H(z)$ + *BBN* data gives a tighter constraint than the *WMAP9* + *BAO* + $H(z)$ + *BBN* data.

5.2.1 The Dark Radiation

Again, as Table 2 hints, the *SNLS* data is not sensitive to the effective neutrino number. In contrast, the constraints from other data are at much smaller orders. For concise, we only discuss the tightest constraints from Data IV. The combined data favor a positive f which denotes the new produced dark radiation. Based on our definition, the data gives out $N_{eff} = 3.25^{+0.74+1.00}_{-0.68-0.88}$ in flat dark radiation model and $N_{eff} = 3.09^{+1.17+1.53}_{-0.97-1.18}$ in the curved one. Dark radiation makes the best fit of N_{eff} slightly larger than 3.04. We compare the flat and curved cases by drawing the contours of H_0 and N_{eff} in Figure 3 where the ranges of H_0 are nearly the same, but the range of N_{eff} is larger in the curved case.

5.2.2 The Om Diagnostic

The Om diagnostic is used to distinguish the dark radiation effect. For our model,

$$Om(x) = \Omega_{m0} + \frac{(\Omega_{r0} + \Omega_{dr0})(x^2 + 1)(x + 1)}{x^2 + x + 1} + \frac{\Omega_{k0}(1 + x)}{x^2 + x + 1}. \quad (25)$$

Generally, the effect of today's dark radiation makes $\delta Om_{dr0} < 4\Omega_{dr0}/3$. Meanwhile, the effect of today's curvature makes $\delta Om_{k0} < \Omega_{k0}/2$. As f (or Ω_{dr0}) are relative small, δOm_{dr0} is smaller than δOm_{k0} . Robustly, Ω_{dr0} ($\sim 10^{-5}$) is four orders smaller than Ω_{m0} (10^{-1}) and three order smaller than Ω_{k0} (10^{-2}). The relation of $Om - z$ are drawn out in Figure 4 for the flat and curved dark radiation cases. In the flat one, the best fitting value of Om is nearly constant, so does its 1σ and 2σ ranges. But the behavior of Om in the curved Λ CDM model and the curved dark radiation model show dynamical signals. Considering the flat Λ CDM model which gives a constant Om [52] as well, the flat dark radiation model could not be distinguished from the flat Λ CDM model while the curved dark radiation model can.

5.2.3 Parameter Degeneration

Figure 5 presents the contours of $\Omega_{m0} - f$, $\Omega_{k0} - f$ and $\Omega_{m0} - \Omega_{k0}$ of the flat and curved dark radiation models given by different datasets. As we mentioned above, the *SNLS* data give

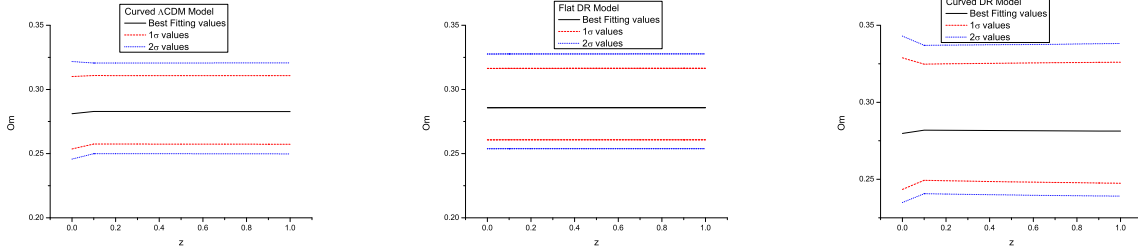


Figure 4: The Om diagnostic for the curved Λ CDM model, the flat and curved dark radiation models are give out.

out loose constraints. Meanwhile, the three data (DataII, III and IV) give much tighter constraints which also have the same contour directions. For the contour of $\Omega_{m0} - \Omega_{k0}$, all the data give the same constrain direction. In contrast, for $\Omega_{m0} - f$ and $\Omega_{k0} - f$, the SNLS data and the other data gives contours with different directions. Obviously, the degeneration between the dark radiation parameter f and the other parameters need more data to break.

6 The Summary

Theoretically, after adding dark radiation, the phase-analysis method proved that the universe derived from the dark radiation model could go through the radiation dominated phase, the matter dominated phase and the dark energy dominated phase sequently. In a conclusion, the model is compatible with the history of our universe.

Observationally, we use the *SNLS*, *WMAP9*, *PLANCK*, *BAO*, $H(z)$ and *BBN* data to constrain the dark radiation part. As expected, the dark radiation wiped out the tension between the *SNLS* data and the other data in flat Λ CDM model. And, the constraining results are at a reasonable level, e.g. $f \sim 10^{-5}$. The small dark radiation parameter f give a small deviation of ω_0 and ω'_0 . And, the effect of dark radiation make the best fit value of N_{eff} slightly larger than 3.04. Anyway, the Om diagnostic could extract the curved dark radiation from the flat Λ CDM model, but it has no effect on the flat dark radiation model. And, more data are needed for dark radiation because of parameter degenerations.

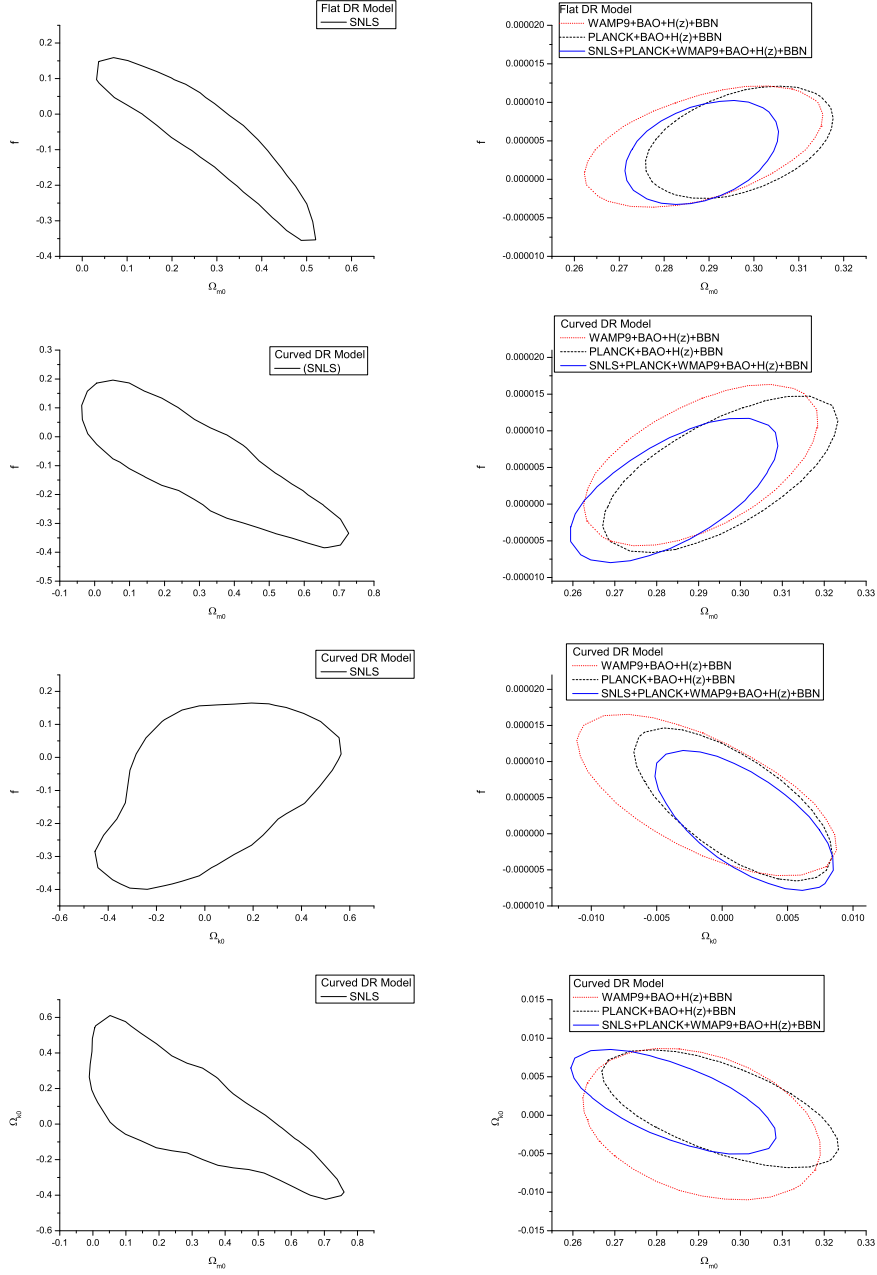


Figure 5: The 1σ parameter contours given by different data are presented.

7 Acknowledgements

We are grateful to the useful suggestions from the anonymous referee. YZ thanks the useful discussion with Dr. Hao Wang, Dr. Hongbo Zhang, Dr. Yu Pan, Prof. Nana Pan. This work was supported by the Ministry of Science and Technology of China national basic science Program (973 Project) under grant Nos. 2010CB833004, the National Natural Science Foundation of China project under grant Nos. 11175270, 11005164, 11073005 and 10935013, CQ CSTC under grant No. 2010BB0408, and CQ MEC under grant No. KJTD201016. Part of this research was supported under the U.S. Department of Energy contract DE-AC02-06CH11357 and by the DOE under contract W-7405-ENG-36.

References

- [1] A.G. Riess et al., *AJ*. **116**, 1009 (1998).
- [2] S. Perlmutter et al., *ApJ* **517**, 565 (1999).
- [3] J. L. Tonry et al., *ApJ* **594**, 1 (2003).
- [4] R.A. Knop et al., *ApJ* **598**, 102 (2003).
- [5] A.G. Riess et al., *ApJ* **607**, 665 (2004).
- [6] C.L. Bennet et al., *ApJS*. 148, 1 (2003).
- [7] D.N. Spergel et al., *ApJS*, 148, 175 (2003); D.N. Spergel et al., *ApJS* **170**, 377 (2007).
- [8] L. Page et al., *ApJS* **170**, 335 (2007).
- [9] G. Hinshaw et al., *ApJS* **170**, 263 (2007).
- [10] E. Komatsu *et al.* [WMAP Collaboration], *Astrophys. J. Suppl.* **192**, 18 (2011) [arXiv:1001.4538 [astro-ph.CO]].
- [11] L. Randall and R. Sundrum, *Phys. Rev. Lett.* **83**, 3370 (1999) [arXiv:hep-ph/9905221].
- [12] R. G. Vishwakarma and P. Singh, *Class. Quant. Grav.* **20**, 2033 (2003) [arXiv:astro-ph/0211285].

- [13] K. Ichiki, M. Yahiro, T. Kajino, M. Orito and G. J. Mathews, Phys. Rev. D **66**, 043521 (2002) [arXiv:astro-ph/0203272].
- [14] K. Ichiki, P. M. Garnavich, T. Kajino, G. J. Mathews and M. Yahiro, Phys. Rev. D **68**, 083518 (2003) [arXiv:astro-ph/0210052].
- [15] E. Calabrese, D. Huterer, E. V. Linder, A. Melchiorri and L. Pagano, Phys. Rev. D **83** (2011) 123504 [arXiv:1103.4132 [astro-ph.CO]].
- [16] A. De Felice, G. Mangano, P. D. Serpico and M. Trodden, Phys. Rev. D **74**, 103005 (2006) [arXiv:astro-ph/0510359].
- [17] S. Dutta and E. N. Saridakis, JCAP **1001** (2010) 013 [arXiv:0911.1435 [hep-th]].
- [18] A. Ali, S. Dutta, E. N. Saridakis and A. A. Sen, Gen. Rel. Grav. **44**, 657 (2012) [arXiv:1004.2474 [astro-ph.CO]].
- [19] J. A. S. Lima, A. I. Silva and S. M. Viegas, Mon. Not. Roy. Astron. Soc. **312**, 747 (2000).
- [20] M. Birkel and S. Sarkar, Astropart. Phys. **6**, 197 (1997) [arXiv:astro-ph/9605055].
- [21] J. A. S. Lima, Phys. Rev. D **54**, 2571 (1996) [arXiv:gr-qc/9605055].
- [22] M. Bordag, U. Mohideen and V. M. Mostepanenko, Phys. Rept. **353**, 1 (2001) [arXiv:quant-ph/0106045].
- [23] J. Dunkley *et al.*, Astrophys. J. **739**, 52 (2011) [arXiv:1009.0866 [astro-ph.CO]].
- [24] S. Das *et al.*, arXiv:1301.1037; R. Keisler *et al.*, ApJ 74328(2011); C.L.Reichardt *et al.*, ApJ 763,127(2013); 26 C. L. Reichardt *et al.*, ApJ 755, 70 (2012); K. T. Story *et al.*, arXiv:1210.7231.
- [25] R. Keisler, C. L. Reichardt, K. A. Aird, B. A. Benson, L. E. Bleem, J. E. Carlstrom, C. L. Chang and H. M. Cho *et al.*, Astrophys. J. **743**, 28 (2011) [arXiv:1105.3182 [astro-ph.CO]].
- [26] R. H. Cyburt, B. D. Fields, K. A. Olive and E. Skillman, Astropart. Phys. **23**, 313 (2005) [arXiv:astro-ph/0408033].
- [27] W. Fischler and J. Meyers, Phys. Rev. D **83**, 063520 (2011) [arXiv:1011.3501 [astro-ph.CO]].

- [28] Y. Zhang, H. Li, Y. Gong and Z. -H. Zhu, *Eur. Phys. J. C* **72**, 2035 (2012).
- [29] J. Hamann, *JCAP* **1203**, 021 (2012) [arXiv:1110.4271 [astro-ph.CO]].
- [30] J. L. Menestrina and R. J. Scherrer, *Phys. Rev. D* **85**, 047301 (2012) [arXiv:1111.0605 [astro-ph.CO]].
- [31] S. Dutta, S. D. H. Hsu, D. Reeb and R. J. Scherrer, *Phys. Rev. D* **79** (2009) 103504 [arXiv:0902.4699 [astro-ph.CO]].
- [32] A. Conley *et al.*, *Astrophys. J. Suppl.* **192**, 1 (2011) [arXiv:1104.1443 [astro-ph.CO]].
- [33] M. Sullivan *et al.*, *Astrophys. J.* **737**, 102 (2011) [arXiv:1104.1444 [astro-ph.CO]].
- [34] C. L. Bennett, D. Larson, J. L. Weiland, N. Jarosik, G. Hinshaw, N. Odegard, K. M. Smith and R. S. Hill *et al.*, arXiv:1212.5225 [astro-ph.CO].
- [35] G. Hinshaw *et al.* [WMAP Collaboration], arXiv:1212.5226 [astro-ph.CO].
- [36] P. A. R. Ade *et al.* [Planck Collaboration], arXiv:1303.5077 [astro-ph.CO].
- [37] W. J. Percival, S. Cole, D. J. Eisenstein, R. C. Nichol, J. A. Peacock, A. C. Pope and A. S. Szalay, *Mon. Not. Roy. Astron. Soc.* **381**, 1053 (2007) [arXiv:0705.3323 [astro-ph]].
- [38] W. J. Percival *et al.* [SDSS Collaboration], *Mon. Not. Roy. Astron. Soc.* **401**, 2148 (2010) [arXiv:0907.1660 [astro-ph.CO]].
- [39] C. Blake *et al.*, *Mon. Not. Roy. Astron. Soc.* **418**, 1707 (2011) [arXiv:1108.2635 [astro-ph.CO]].
- [40] F. Beutler *et al.*, *Mon. Not. Roy. Astron. Soc.* **416**, 3017 (2011) [arXiv:1106.3366 [astro-ph.CO]].
- [41] J. Simon, L. Verde and R. Jimenez, *Phys. Rev. D* **71**, 123001 (2005) [arXiv:astro-ph/0412269].
- [42] A. G. Riess *et al.*, *Astrophys. J.* **699**, 539 (2009) [arXiv:0905.0695 [astro-ph.CO]].
- [43] P. Serra, A. Cooray, D. E. Holz, A. Melchiorri, S. Pandolfi and D. Sarkar, *Phys. Rev. D* **80**, 121302 (2009) [arXiv:0908.3186 [astro-ph.CO]].
- [44] S. Burles, K. M. Nollett and M. S. Turner, *Astrophys. J.* **552**, L1 (2001) [arXiv:astro-ph/0010171].

- [45] G. Steigman, *Int. J. Mod. Phys. E* **15**, 1 (2006) [arXiv:astro-ph/0511534].
- [46] A. A. Coley, gr-qc/9910074.
- [47] J. Wainwright and G. F. R. Ellis, *Dynamical Systems in Cosmology*, Cambridge Univ. Press, Cambridge, 1997.
- [48] A. A. Coley, *Dynamical Systems and Cosmology*, in Series: Astrophysics and Space Science Library, Vol. 291, Springer, 2004.
- [49] D. J. Eisenstein and W. Hu, *Astrophys. J.* **496**, 605 (1998) [arXiv:astro-ph/9709112].
- [50] L. Hui and P. B. Greene, *Phys. Rev. D* **73**, 123526 (2006) [arXiv:astro-ph/0512159].
- [51] W. Hu and N. Sugiyama, *Astrophys. J.* **471**, 542 (1996) [arXiv:astro-ph/9510117].
- [52] V. Sahni, A. Shafieloo and A. A. Starobinsky, *Phys. Rev. D* **78**, 103502 (2008) [arXiv:0807.3548 [astro-ph]].
- [53] A. Shafieloo, V. Sahni and A. A. Starobinsky, *Phys. Rev. D* **86** (2012) 103527 [arXiv:1205.2870 [astro-ph.CO]].
- [54] W. Godlowski and M. Szydlowski, *Phys. Lett. B* **642**, 13 (2006) [arXiv:astro-ph/0606731].
- [55] G. Mangano, A. Melchiorri, O. Mena, G. Miele and A. Slosar, *JCAP* **0703**, 006 (2007) [arXiv:astro-ph/0612150].
- [56] S. Bashinsky and U. Seljak, *Phys. Rev. D* **69**, 083002 (2004) [arXiv:astro-ph/0310198].
- [57] M. Archidiacono, E. Calabrese and A. Melchiorri, *Phys. Rev. D* **84**, 123008 (2011) [arXiv:1109.2767 [astro-ph.CO]].
- [58] C. Clarkson, M. Cortes and B. A. Bassett, *JCAP* **0708**, 011 (2007) [astro-ph/0702670 [ASTRO-PH]].
- [59] P. M. Okouma, Y. Fantaye and B. A. Bassett, *Phys. Lett. B* **719**, 1 (2013) [arXiv:1207.3000 [astro-ph.CO]].
- [60] Y. Wang, C. -H. Chuang and P. Mukherjee, *Phys. Rev. D* **85**, 023517 (2012) [arXiv:1109.3172 [astro-ph.CO]].

- [61] Y. Wang and S. Wang, arXiv:1304.4514 [astro-ph.CO].
- [62] H. Akaike, IEEE Trans. Auto. Control. **19**, 716 (1974).
- [63] A. R. Liddle, Mon. Not. Roy. Astron. Soc. **351**, L49 (2004) [arXiv:astro-ph/0401198].

	Flat Λ CDM	Curved Λ CDM	Flat DR Model	Curved DR Model
Data I: <i>SNLS</i>				
Ω_{m0}	$0.226^{+0.039+0.070}_{-0.037-0.070}$	$0.174^{+0.138+0.222}_{-0.154-0.169}$	$0.297^{+0.306+0.383}_{-0.292-0.292}$	$0.145^{+0.832+0.835}_{-0.138-0.140}$
f	—	—	$-0.68^{+0.51+0.90}_{-0.12-0.93}$	$0.22^{0.15+0.19}_{-0.74-0.90}$
Ω_{k0}	—	$0.150^{+0.41+0.59}_{-0.36-0.56}$	—	$0.17^{+0.52+0.62}_{-0.82-0.88}$
$N_{eff}(10^4)$	—	—	$-0.36^{+1.61+1.91}_{-1.34-1.65}$	$0.12^{+1.06+1.54}_{-2.78-2.78}$
χ^2	420.10	419.77	418.60	419.78
<i>AIC</i>	422.10	423.77	422.60	425.78
Data II: <i>WMAP9 + BAO + H(z) + BBN</i>				
Ω_{m0}	$0.280^{+0.029+0.044}_{-0.025-0.036}$	$0.280^{+0.034+0.050}_{-0.028-0.039}$	$0.286^{+0.040+0.059}_{-0.033-0.045}$	$0.287^{+0.049+0.070}_{-0.038-0.051}$
$f(10^{-5})$	—	—	$0.37^{+1.13+1.63}_{-1.04-1.49}$	$0.45^{+1.83+2.63}_{-1.60-2.14}$
$\Omega_{k0}(10^{-2})$	—	$0.18^{+0.99+1.40}_{-0.93-1.31}$	—	$-0.09^{+1.46+1.97}_{-1.55-2.19}$
H_0	$70.19^{+2.21+3.31}_{-2.29-3.40}$	$70.43^{+2.86+4.02}_{-2.88-4.11}$	$70.73^{+3.04+4.35}_{-3.05-4.27}$	$70.74^{+3.38+4.62}_{-3.43-4.67}$
N_{eff}	—	—	$3.28^{+0.72+1.04}_{-0.65-0.92}$	$3.33^{+1.16+1.63}_{-0.10-1.32}$
χ^2	10.17	9.95	9.55	9.54
<i>AIC</i>	12.17	13.95	13.55	15.54
Data III: <i>PLANCK + BAO + H(z) + BBN</i>				
Ω_{m0}	$0.290^{+0.024+0.036}_{-0.020-0.030}$	$0.286^{+0.290+0.417}_{-0.024-0.333}$	$0.296^{+0.030+0.044}_{-0.026-0.037}$	$0.292^{+0.047+0.068}_{-0.039-0.050}$
$f(10^{-5})$	—	—	$0.44^{+1.00+1.43}_{-0.98-1.42}$	$0.29^{+1.78+2.55}_{-1.48-2.01}$
$\Omega_{k0}(10^{-2})$	—	$0.30^{+0.69+0.97}_{-0.71-1.02}$	—	$0.17^{+1.05+1.38}_{-1.29-1.81}$
H_0	$69.46^{+1.75+2.60}_{-1.81-2.67}$	$70.35^{+2.76+3.94}_{-2.90-4.11}$	$70.31^{+2.95+4.15}_{-2.80-4.01}$	$70.46^{+3.38+4.56}_{-3.29-4.54}$
N_{eff}	—	—	$3.32^{+0.65+0.93}_{-0.60-0.84}$	$3.23^{+1.09+1.54}_{-0.92-1.24}$
χ^2	10.73	9.84	9.71	9.62
<i>AIC</i>	12.73	13.84	13.71	15.62
Data IV: <i>SNLS + WMAP9 + PLANCK + BAO + H(z) + BBN</i>				
Ω_{m0}	—	$0.281^{+0.029+0.041}_{-0.027-0.035}$	$0.286^{+0.031+0.042}_{-0.025-0.032}$	$0.280^{+0.049+0.063}_{-0.036-0.045}$
$f(10^{-5})$	—	—	$0.31^{+1.10+1.50}_{-1.11-1.46}$	$0.08^{+1.82+2.43}_{-1.53-1.86}$
$\Omega_{k0}(10^{-2})$	—	$0.26^{+0.75+0.95}_{-0.77-1.07}$	—	$0.32^{+0.95+1.24}_{-1.40-1.81}$
H_0	—	$70.65^{+3.39+4.25}_{-3.10-4.09}$	$70.78^{+3.24+4.17}_{-3.42-4.49}$	$71.11^{+3.45+4.45}_{-3.90-5.01}$
N_{eff}	—	—	$3.25^{+0.74+1.00}_{-0.68-0.88}$	$3.09^{+1.17+1.53}_{-0.97-1.18}$
χ^2	—	433.62	433.86	433.66
<i>AIC</i>	—	437.62	437.86	439.66

Table 2: The maximum likelihood values with 1σ and 2σ confidence ranges are presented for the flat Λ CDM model, the curved Λ CDM model, the flat Λ CDM model with dark radiation (Flat DR Model) and the curved Λ CDM model with dark radiation (Flat DR Model).